EUROPEAN ORGANIZATION FOR NUCLEAR RESEARCH

CERN – AB DIVISION

AB-Note-2003-092 (OP)

Study of the Optics Parameters in the LT-LTB-BI Transfer Line

K. Hanke, J. Sanchez-Conejo

Abstract

The Twiss parameters and dispersion in the Linac II to Booster transfer line (LT-LTB-BI) have been measured during the 2003 run. For the Twiss parameters we find very good agreement between simulation and measurement. Furthermore, the line appears to be very well matched at the Booster injection point. Also for the dispersion, we find very good agreement of simulation and measurements. We have computed and experimentally tested a new optics, which nullifies the dispersion and dispersion derivative in the last part of the line (achromatic line). Although such a solution exists on paper, it was found that good transmission and minimised dispersion are conflicting constraints.

Geneva, Switzerland

February 6, 2004

1 Introduction

The LT-LTB-BI line links the CERN Linac II to the CERN PS Booster (PSB). While the first part (LT) is only used for protons coming from Linac II, the second (LTB) and third (BI) parts of the line are common to protons and ions coming from Linac III. In order to allow for this dual purpose, the LT part of the line comprises two horizontal bending magnets (LT.BHZ20 and LT.BHZ30). Figure 1 shows schematically the line and its main elements. The optics in operation during the 2003 run is given in Table. 1.

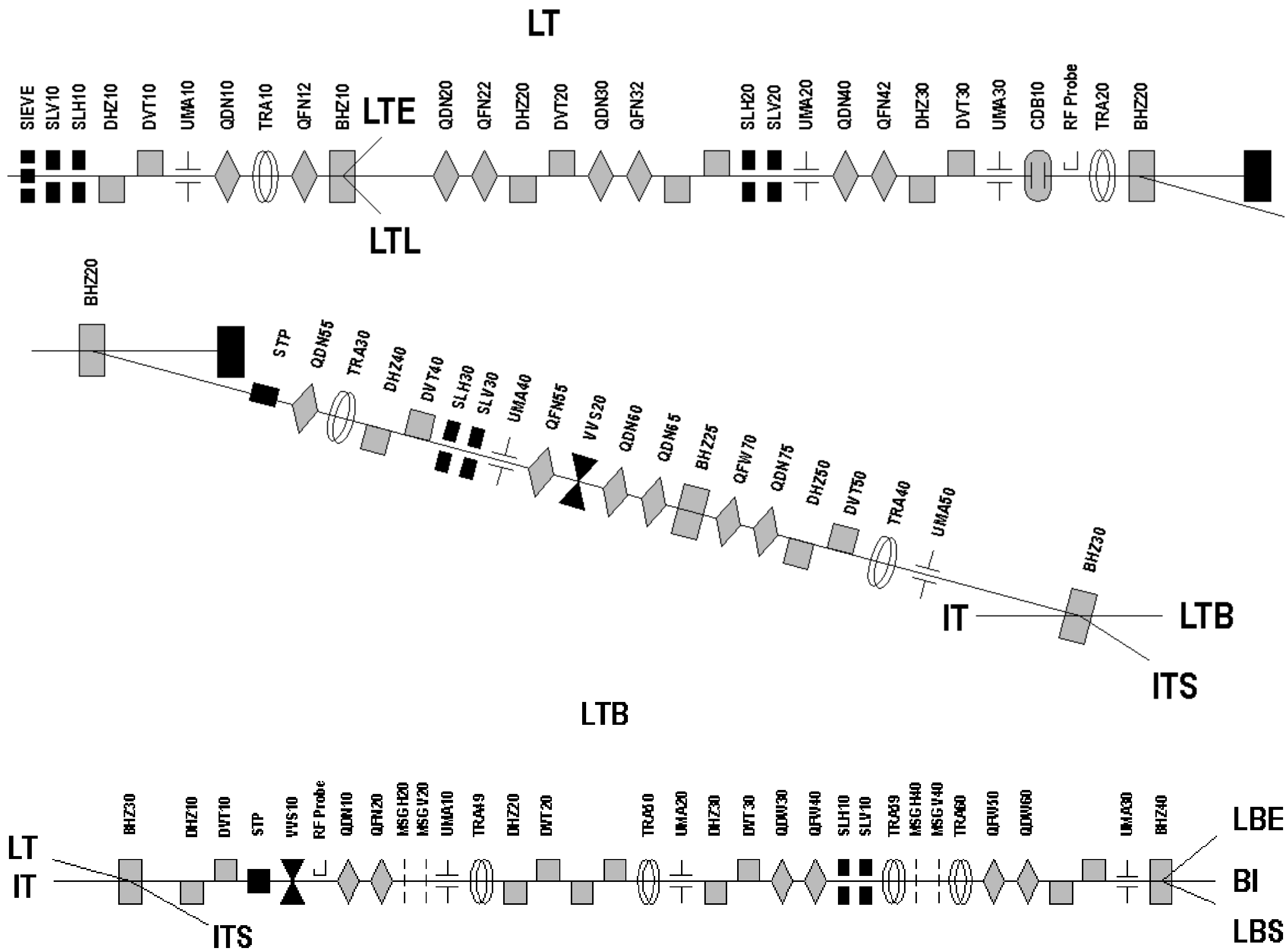

Figure 1: Schematic lay-out of the LT-LTB-BI transfer line. Top: straight part of the LT line; middle: part of the LT line between horizontal bending magnets; bottom: LTB line.

We have worked with a 160 to 170 mA proton beam at 50 MeV (user "MDLHC"). The beam is initially space-charge dominated, while the effect of space charge becomes less important as the beam debunches along the line. During our experiments, we have injected beam only into ring 3 of the Booster. The target match at injection into the PS Booster is given in Table 2.

element	current [A] (ccv value)
LT.QDN10	293.00
LT.QFN12	230.00
LT.QDN20	130.00
LT.QFN22	90.00
LT.QDN30	44.20
LT.QFN32	73.00
LT.QDN40	118.50
LT.QFN42	97.10
LT.QDN50	45.70
LT.QFN55	52.40
LT. QDN60 + 65	34.80
LT.QFW70	-7.50
LT.QDN75	41.00
LTB.QDN10	63.00
LTB.QFN20	38.00
LTB.QDW30	-11.50
LTB.QFW40	11.10
LTB.QFW50	-10.00
LTB.QDW60	10.00
BI.QNO10	16.50
BI.QNO20	19.20
BI.QNO30	10.70
BI.QNO40	14.40
BI1.QNO50	47.50
BI1.QNO60	54.50
BI2.QNO50	49.00
BI2.QNO60	54.00
BI3.QNO50	52.00
BI3.QNO60	56.50
BI4.QNO50	50.00
BI4.QNO60	56.50

Table 1: CCV values of the quadrupoles in the LT, LTB and BI lines for the operational optics in 2003.

	horizontal	vertical
α	0.0	0.0
β [m]	2.0[1]	2.7
D [m]	1.42	0.0
D'	0.0	0.0

Table 2: Target match at injection into the PS Booster.

[1)] The value of the horizontal β-function in the Booster ring at this point is 5.6 m.

2 Twiss Parameters

For the Twiss parameter matching, we have used reference files for the simulation code *TRACE*, which had previously been checked versus transfer matrix measurements [1]. *TRACE* takes into account space charge as a defocussing force, which is calculated for each element. Figure 2 shows a simulation of the line using *TRACE* for the operational optics and 160 mA beam current. The horizontal and vertical envelope, the horizontal dispersion as well as the position of the bending magnets are shown.

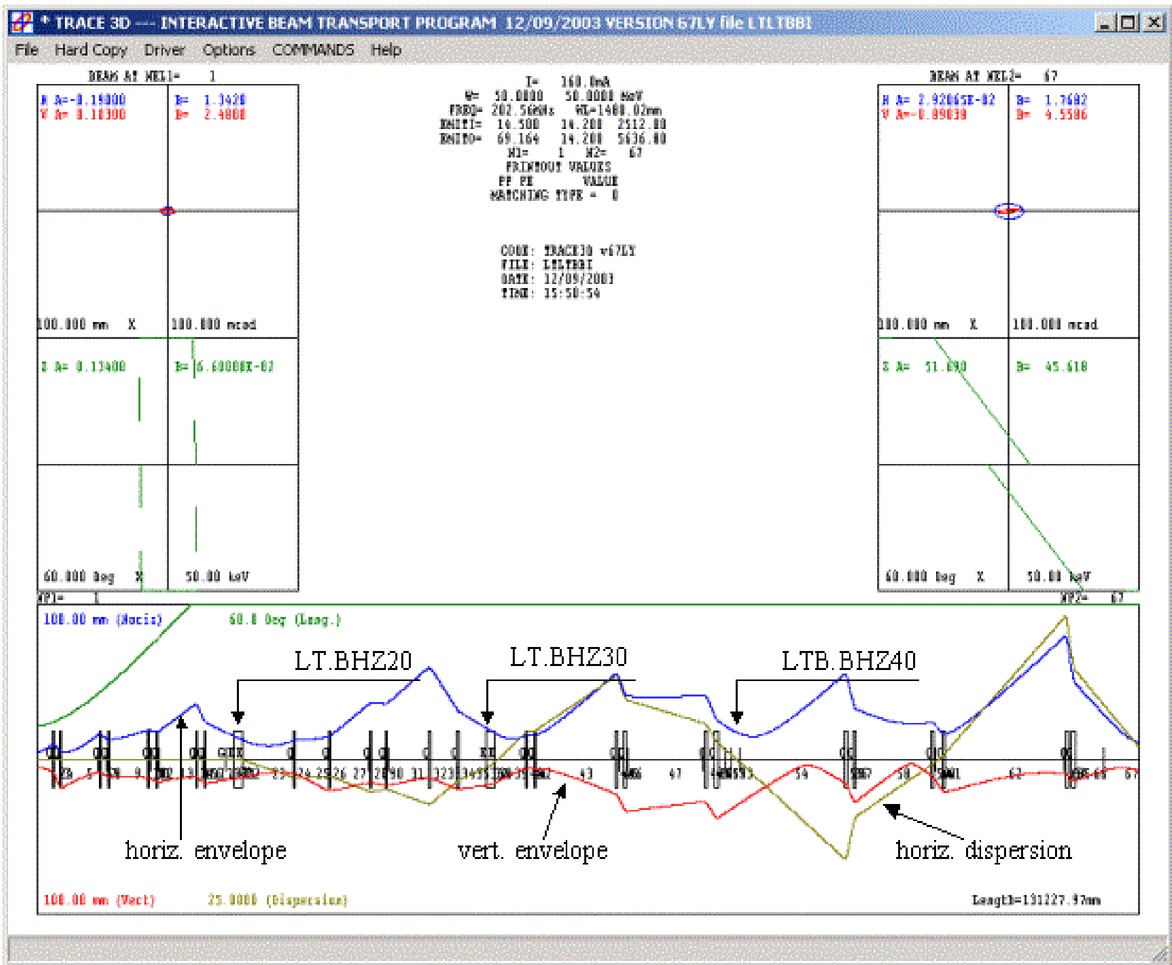

Figure 2: TRACE simulation of the LT-LTB-BI line with the operational optics and 160 mA beam current. The horizontal and vertical envelope as well as the horizontal dispersion are displayed. The position of the bending magnets is indicated. The scale of the dispersion is $\pm$ 25 m, the scale of the envelopes is 100 mm.

The Twiss parameters α and β have been measured in both planes using a dedicated emittance measurement line (LBE). The beam is deflected into this line using the bending magnet LTB.BHZ40 (see Figure 1). In the LBE line, the beam is swept over a slit. The particles passing through the slit are detected by a secondary emission (SEM) grid. This procedure yields a direct image of the beam in phase space. Figure 3 shows a typical measurement of the horizontal Twiss parameters in the LBE line.

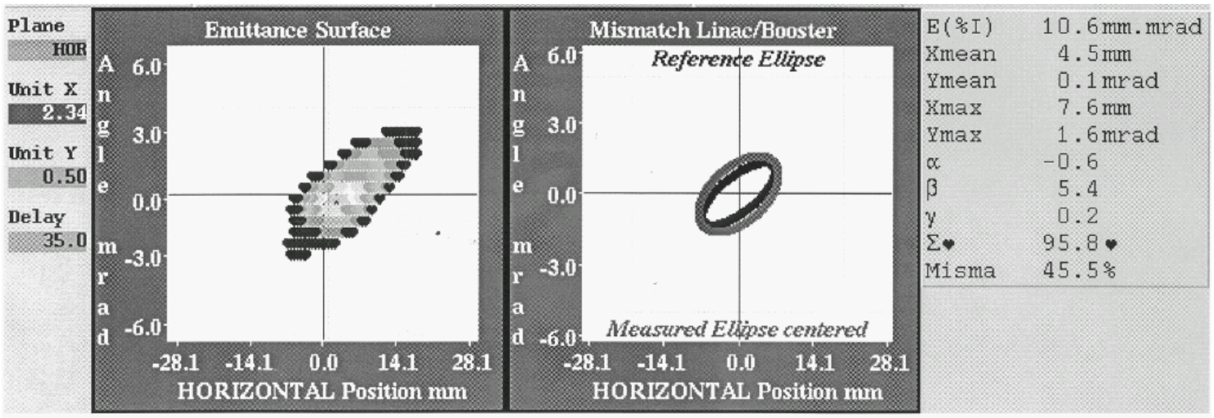

Figure 3: Typical measurement of horizontal Twiss parameters in the LBE measurement line. The same technique applies to the vertical plane.

The Twiss parameters at the location of the slit are obtained from a fit in the phase space. As the beam is space-charge dominated, the Twiss parameters cannot simply be transported back to the point of interest by matrix multiplication or tracking. Such a procedure would not treat the effect of space charge correctly, as the beam blow-up would be reversed. Instead, a matching has to be performed, where the initial beam parameters at the entry of LTB.BHZ40 are varied until the measured values at the slit location are reproduced. Figure 4 illustrates the procedure. In a first step, a matching procedure is performed, in which the Twiss parameters at the entry plane of LTB.BHZ40 are used as free parameters and varied until the measured Twiss parameters at the slit location are reproduced. Having found the right set of parameters at the entry plane of the bending magnet, these can be used as input conditions for a simulation of the part of the line starting from LTB.BHZ40 to the Booster injection point.

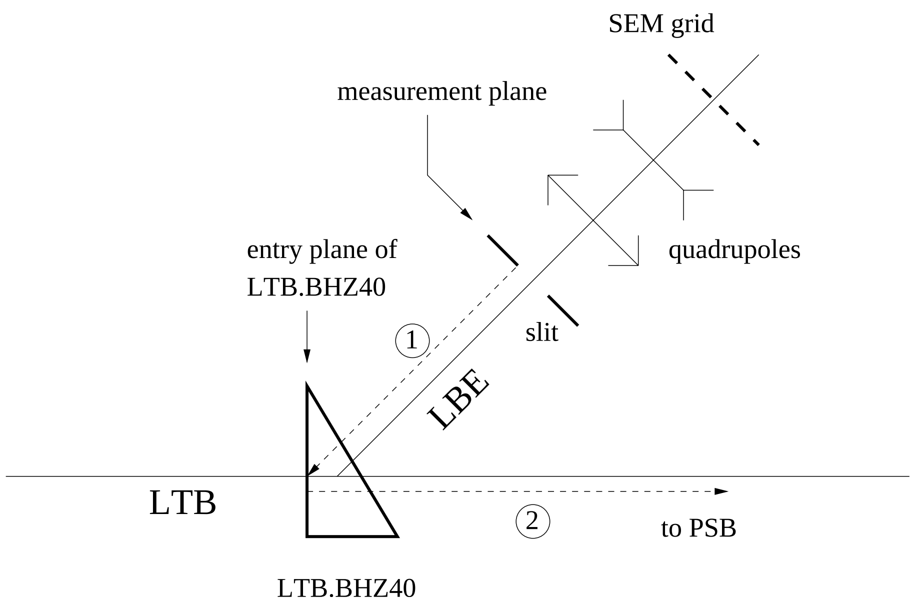

Figure 4: Principle of obtaining the Twiss parameters at the entry plane of LTB.BHZ40 from a measurement in the LBE line. In a first step, the Twiss parameters at the entry plane of the dipole are varied until the measured parameters at the slit location are reproduced. In a second step, the solution found at the entry plane of the dipole can be used as input conditions for a simulation of the line, starting at LTB.BHZ40 to the Booster injection point.

Table 3 shows the measured Twiss parameters at the location of the slit as well as the corresponding parameters at the entry plane of LTB.BHZ40. The values are averaged over a series of measurements. Using the Twiss parameters at the entry of LTB.BHZ40 as initial conditions, we have simulated the BI line from LTB.BHZ40 to the injection point into the PS Booster. The results are also given in Table 3.

location	α_x	β_x [m]	α_y	β_y [m]
at LBE slit	-0.58	6.98	1.8	7.56
entry of LTB.BHZ40	2.88	19.97	15.60	96.85
PSB injection point	0.12	2.33	-0.12	2.63

Table 3: Twiss parameters measured in the LBE line and corresponding values at the entry of LTB.BHZ40 (for I=160 mA).

As can bee seen, the Twiss parameters are already in good agreement with the target match given in Table 2. We have, nevertheless, tried a re-matching of the line, in order to reproduce exactly the target match. *TRACE* easily converges to such a solution. However, loading the re-matched optics to the machine did not improve the performance. We conclude, that the present optics of the line is close to a perfectly matched solution with respect to the Twiss parameters. Even if there is some slight discrepancy between the measured Twiss parameters at injection according to Table 3 and the target match given in Table 2, the present operational optics appears to be empirically so well optimised that we could not find any improvement.

3 Dispersion

The simulation of the dispersion function along the line does not rely on the measurement of the initial conditions, as it can be assumed that in both planes dispersion and dispersion derivative are zero at the entry of the line. The simulation is however complicated by the presence of space charge. While a particle in the beam center is not affected by space charge (assuming a symmetrical beam), particles outside the center do see an effect of space charge. We distinguish therefore space charge dependent dispersion and space charge independent dispersion. We consider in the following the space charge independent dispersion, as this quantity is accessible to our measurements.

Both *TRACE*, which is able to take into account space charge, as well as *MAD*, which does not take into account space charge, have been used to simulate the dispersion function along the line. Figure 5 shows the horizontal dispersion function along the line as computed with *MAD* for the original optics. As can be seen from Figure 5, the dispersion function is zero in the first part of the line and starts to become non-zero at the location of the first horizontal bending magnet, LT.BHZ20 (entry plane of the magnet at 23.56 m). At the location of the second bending magnet, LT.BHZ30 (entry plane of the magnet at 53.55 m), the dispersion is close to zero while the dispersion derivative is not. Consequently, the dispersion function oscillates through the quadrupole lattice of the line ending up with non-zero values for both dispersion and dispersion derivative at the Booster injection point.

Although the target match for the horizontal dispersion has a finite value of 1.42 m (see Table 2, we have aimed at an optics, where $D_x = D'_x = 0$ at the exit of LT.BHZ30. Such an achromatic line has the advantage, that the part of the line downstream of LT.BHZ30 is completely robust against energy fluctuations, both in terms of trajectory and beam size. Furthermore, all magnets in this area can be tuned in order to re-match the Twiss parameters (which are unavoidably changed during the dispersion matching) without affecting the dispersion at the same time.

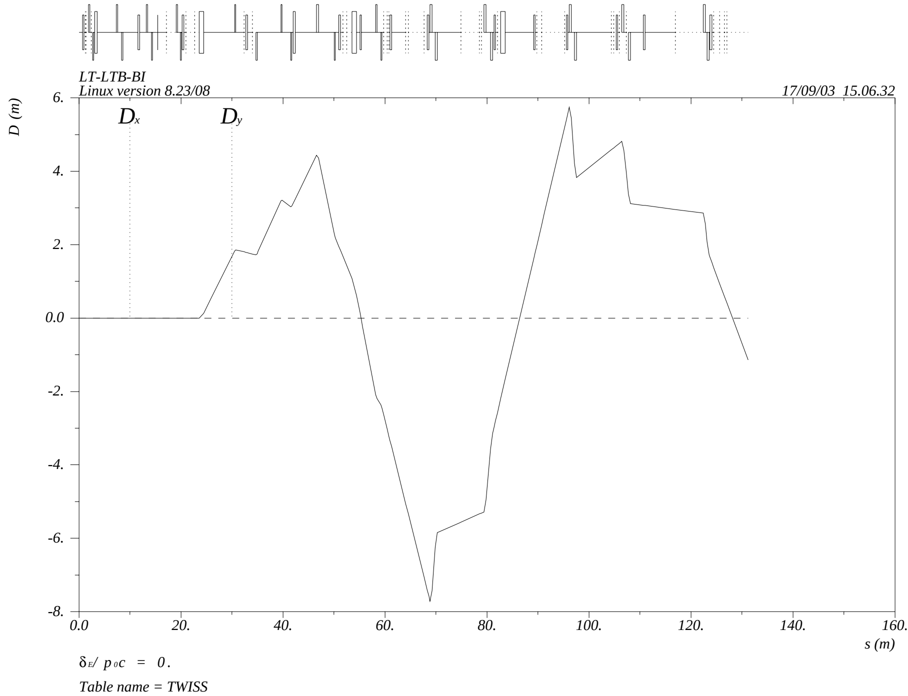

Figure 5: Horizontal dispersion function versus length as calculated with *MAD* for the operational optics. The dispersion function is zero in the first part of the line, and starts to become non-zero at the location of LT.BHZ20 (23.56 m).

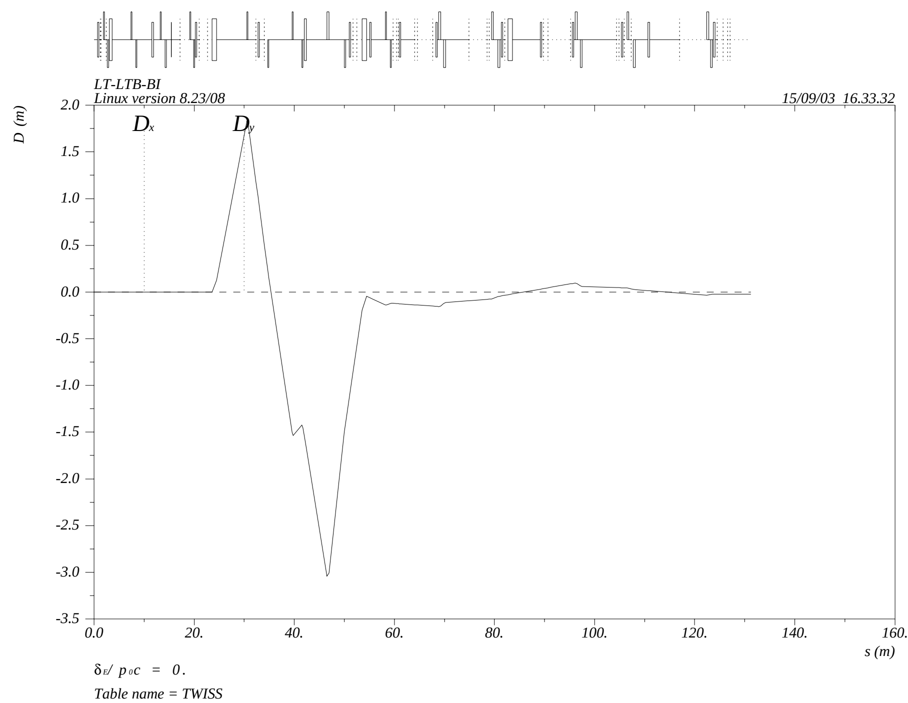

Figure 6: Horizontal dispersion function versus length as calculated with *MAD* for the re-matched optics. The dispersion as well as the dispersion derivative are close to zero at the exit of LT.BHZ30 and remain zero until the Booster injection point.

By using quadrupoles downstream of LT.BHZ30 for dispersion matching, one can only trade off D versus D', but not nullify both. To match an optics, which nullifies both the dispersion and the dispersion derivative at the exit of the second bending magnet (achromatic line), quadrupoles between the bending magnets LT.BHZ20 and LT.BHZ30 have to be varied. We have found, that the two quadrupoles LT.QFN50 and LT.QFW70 are efficient knobs to tune the dispersion. Using mainly these two quadrupoles, we have found an achromatic optics for the line. Figure 6 shows the horizontal dispersion along the line as computed with *MAD*.

In order to measure the dispersion, we have changed the beam momentum and observed the displacement of the beam center at the location of the pick-ups in the LT and LTB lines. The energy change can be accomplished by changing the phase of the de-buncher LT.CDB10. Table 4 shows the applied phase settings as well as the corresponding momentum change. We have measured the horizontal dispersion

phase (aqn.) [deg]	Δp [keV/c]
286.9	144.40
292.5	65.12
298.1	0.00
303.8	-56.67
309.4	-125.76
315.0	-157.92
320.6	-202.11
326.2	-243.98
331.9	-268.69
337.5	-270.07

Table 4: Applied phase settings for LT.CDB10 and corresponding beam momentum shift (from [2]).

at the location of the pick-ups in the LT and LTB lines for both the original optics as well as for the re-matched optics according to Figure 6. Figure 7shows the measured dispersion for the original optics. In the same figure, the dispersion function as computed with *MAD* is shown. The *MAD* simulation reproduces well the experimental data.

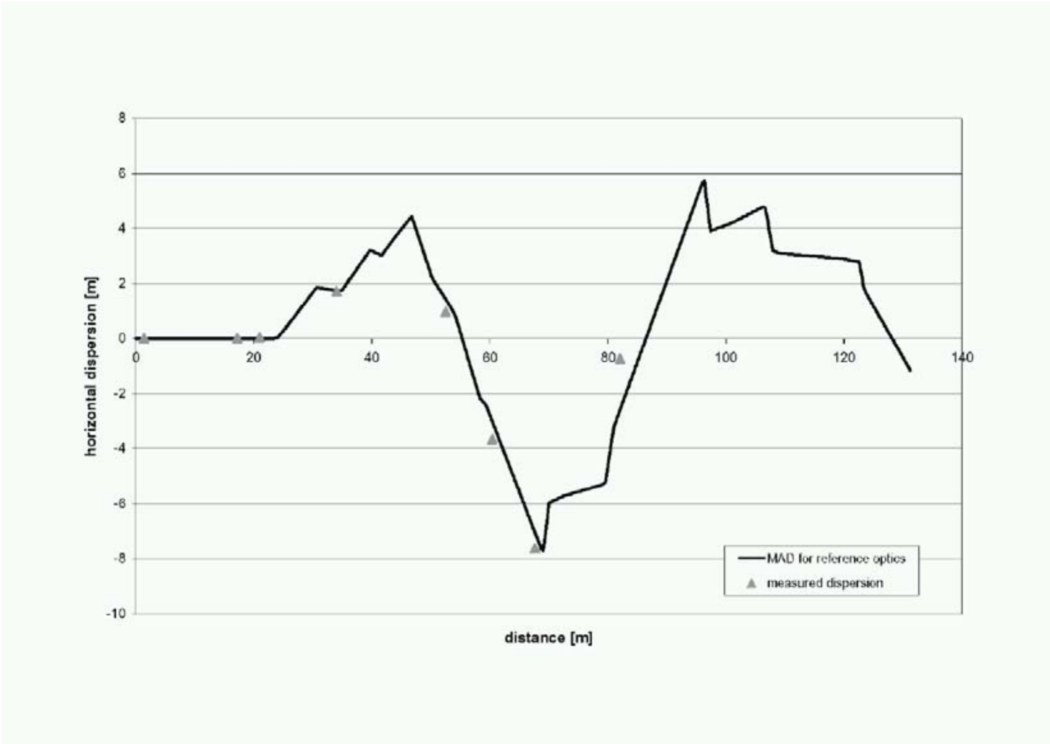

Figure 7: Measured horizontal dispersion at location of LT and LTB pick-ups for the reference optics. The results are in good agreement with a *MAD* simulation (solid line).

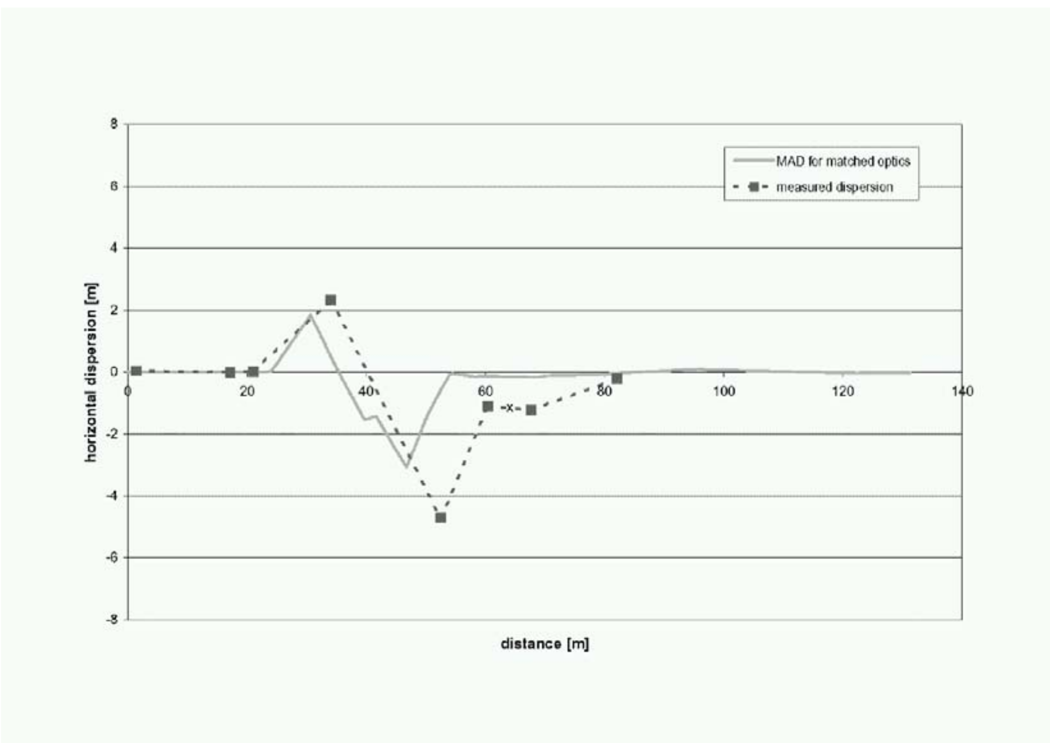

Figure 8: Measured horizontal dispersion at location of LT and LTB pick-ups for the matched optics. The solid line corresponds to the matched optics (see Figure 6). Reasonable agreement could be achieved after manually tuning quadrupoles between the bending magnets.

In earlier measurements [3], the measured values had to be scaled by a factor of 1.75 in order to find agreement with the simulation. We have summarised in Table 5 the experimental data of 2002 and 2003. While the 2003 data agree well with the simulation, the 2002 data have to be scaled in order to achieve

pick-up	measured D_x (2002) [m]	measured D_x (2003) [m]
LT.U10	-0.02154	0.02914
LT.U20	0.00188	0.02615
LT.U30	0.0391	0.05439
LT.U40	0.8866	1.71209
LT.U50	0.24331	0.981172
LTB.U10	-2.10875	-3.64849
LTB.U20	-3.80288	7.61223
LTB.U30	-0.05156	0.71485

Table 5: Experimental results from 2002 compared with those of 2003. The 2003 values agree well with the simulation, while the 2002 values have to be scaled by a factor in order to achieve agreement.

agreement. The reason for this is unclear, as both the experiments and the data analysis have been done in the same way. A possible explanation is, that some quadrupole power supplies have been exchanged during the 2002/2003 shutdown, which leads to a slightly different optics. Another possible explanation is a faulty pick-up read out during the 2002 measurements.

Loading the matched optics to the quadrupoles resulted firstly in a decrease of transmission. Secondly, the measured dispersion did not agree with the *MAD* simulation. After manually tuning quadrupoles between LT.BHZ20 and LT.BHZ30, notably LT.QFN50 and LT.QFW70, we could achieve reasonable agreement of the experimental data with the achromatic optics we were aiming at (Figure 8). It is not clear, why in the case of the operational optics the simulation predicts well the experiment, while in the case of the re-matched optics is does not, A possible explanation might be the effect of space charge, which becomes important as the beam is focused down to small dimensions as it is the case for the achromatic optics. In this case, the *MAD* model may no longer be valid.

In spite of extensive tuning of quadrupoles, we found no setting where the dispersion was nullified, or at least minimised, and at the same time good transmission was conserved. We conclude, that nullifying the dispersion and keeping a good transmission are conflicting constraints. An achromatic line appears to be not feasible with the given quadrupoles respectively quadrupole positions.

4 Conclusions

The measurement campaign performed during the 2003 run yields a complete picture of the optical parameters in the LT-LTB-BI line. The Twiss parameters α and β, measured in the LBE line, are in very good agreement with the simulation. Furthermore, the present optics of the line appears to be very well optimised in terms of Twiss parameter matching.

The measured dispersion is also in good agreement with the experimental data for the operational optics. This is an important result, as in previous studies agreement was only reached introducing artificial factors [3]. A solution for an achromatic line, which exists on paper, was found to be conflicting with good transmission. Furthermore, for this optics, agreement between experimental data and simulation was not satisfactory and manual tuning was required to bring the measured dispersion down to the calculated values. We conclude, that with the given arrangement of quadrupoles, such an optics can in practice not be accomplished.

References

[1] P. Eliasson, K. Hanke, A. Lombardi, J. Sanchez, R. Scrivens, *Study of the LT-LTB Line via Transfer Matrix Measurements*, CERN PS/PP Note 2002-107 (2002).

[2] R. Scrivens, *Beam Momentum Shift Calibration from the Debuncher (LT.CDB10)*, not published.

[3] P. Eliasson, K. Hanke, R. Scrivens, *Dispersion Measurement of 7 August 2002*, not published.